Am J Stem Cells 2026;15(3):81-92
www.AJSC.us /ISSN:2160-4150/AJSC0176390

Original Article

Comparison of physiological functions between limbus niche cells and corneal stromal cells

Mengling Jiang[1,3*], Xinghan Guo[1,2*], Zibin Liu[1,2], Xuying Wang[1,2], Tianyu Zhou[1,2], Lingjuan Xu[1,2], Guigang Li[1,2]

[1]Department of Ophthalmology, Tongji Hospital, Tongji Medical College, Huazhong University of Science and Technology, Wuhan 430030, Hubei, China; [2]Hubei Key Laboratory of Otorhinolaryngologic and Ophthalmic Diseases, Wuhan 430030, Hubei, China; [3]Department of Ophthalmology, Renmin Hospital of Wuhan University, Wuhan 430060, Hubei, China. [*]Equal contributors.

Received August 31, 2026; Accepted October 20, 2026; Epub October 25, 2026; Published October 30, 2026

Abstract: Objective: To systematically compare the physiological functions of limbal niche cells (LNCs) and corneal stromal cells (CSCs), evaluate the feasibility of converting LNCs into CSCs for corneal stromal regeneration, and provide a theoretical basis for cell therapy of corneal ectatic diseases (e.g., keratoconus). Methods: Single-cell RNA sequencing (scRNA-seq) was used to analyze transcriptomic differences among 34,959 cells from human corneal tissues. Morphological changes and expression differences of immunofluorescent markers (Lumican, ALDH1A1, etc.) in the two cell types were observed through in vitro culture. A rabbit transplantation model was employed to assess cell survival, migration, and corneal integration at two and four weeks postoperatively, with histological analyses such as HE staining to verify safety. Results: scRNA-seq revealed significant transcriptomic differences between LNCs and CSCs, with distinct expressions of key markers (THY1, VIM, Lumican) and transcriptional regulators (YAP1/TEAD1). During in vitro culture, CSCs gradually exhibited a spindle-shaped morphology similar to LNCs, and Lumican and ALDH1A1 could serve as effective discriminative markers. In vivo experiments confirmed that both cell types survived long-term (at least 4 weeks) after transplantation; CSCs migrated in a layered pattern, while LNCs formed punctate aggregates, with no inflammation or scarring observed. LNCs retained mesenchymal progenitor markers (CD73, CD90) and demonstrated potential for stromal integration. Conclusion: LNCs possess the potential to differentiate into CSCs. Their transcriptomic characteristics and functional properties support their application value as a precursor for CSC induction, providing experimental evidence and research directions for cell replacement therapy in corneal stromal diseases.

Keywords: Limbal niche cells, corneal stromal cells, single-cell RNA sequencing, corneal stromal regeneration

Introduction

The healthy cornea is a transparent, avascular tissue composed of five layers: the epithelium, Bowman's layer, the stromal, Descemet's membrane, and the endothelium [1]. The corneal epithelium covers the cornea surface and plays a primary role in maintaining corneal transparency. The corneal epithelium periodically sheds and is replaced by new epithelial cells derived from limbal stem cells (LSCs) [2-4]. The normal physiological activity of LSCs relies on the support of the limbal niche [5, 6]. LSCs have been identified in specific regions of the limbus, where they are surrounded and supported by the limbal niche, which is composed of several cell types such as melanocytes, Langerhans cells, macrophages, basement membrane-forming cells, and limbal niche cells (LNCs) [7].

Corneal stromal cells (CSCs) are mesenchymal cells derived from the neural crest. They reside within collagen fiber lamellae of the corneal stroma and form a cellular network through dendritic interconnections. In a healthy cornea, they usually remain in a quiescent state and only undergo self-renewal [8, 9].

LNCs are a group of primitive cells that exhibit functions of vascular endothelial progenitor cells and mesenchymal stem cell progenitors. They can differentiate into vascular endothelial cells, osteoblasts, chondrocytes, and adipo-

https://doi.org/10.62347/MUOR2844

Table 1. Donor cornea information

Cornea	Sex	Age (years)	Preservation	Experiment
1	male	60	Cell culture media (37 °C for 18 days)	LNC scRNA-seq
2	male	71	Cell culture media (37 °C for 18 days)	LNC scRNA-seq
3	female	55	Cell culture media (37 °C for 18 days)	CSC scRNA-seq

cytes, and they express mesenchymal stem cell markers (CD73, CD90, CD105), several neural crest cell markers (p75NTR, Musashi-1, Sox2, Nestin, etc.), as well as other stem cell markers [10, 11]. In addition, compared with bone marrow mesenchymal stem cells (BMMSCs), LNCs express higher levels of mesenchymal stem cell markers, neural crest cell markers, and stem cell factors, and achieve superior therapeutic effects compared with BMMSCs in a rabbit model of corneal alkali burn-induced limbal stem cell deficiency [12]. LNCs and CSCs are respectively located in the stromal layer of the limbus and the transparent corneal area, with anatomically adjacent positions. Some studies suggest that LNCs may be the precursor cells of CSCs [13]. The mesenchymal stem cell properties of LNCs and the expression of neural crest cell markers indicate that LNCs can serve as an important source of stem cells for differentiation into CSCs, which are mesenchymal cells derived from the neural crests.

To further investigate the feasibility of converting LNCs into CSCs, we generated a high-quality single-cell RNA sequencing (scRNA-seq) dataset derived from 34,959 corneal cells isolated from three donors. Using this dataset, we delineated distinct cell populations and constructed a comprehensive cell atlas. Transcriptomic analysis identified subpopulations with diverse functional roles, which may yield novel insights into LNC-to-CSC conversion, offering potential for future treatment of corneal thinning and ectatic disorders such as keratoconus. This dataset identified markers expressed exclusively in populations including CSCs and LNCs. Additionally, complementary in vitro cellular and in vivo animal experiments were performed to assist in validation.

Materials and methods

Human corneal limbal tissues were obtained from three independent donors (two males, one female; age range: 55-71 years) through the Red Cross Eye Bank at Tongji Hospital (Wuhan, China). Donor demographics are summarized in **Table 1**. All tissues were stored in corneal preservation medium at 4°C and used within five days of receipt. The protocol was approved by the Tongji Ethics Committee and was conducted in accordance with the Declaration of Helsinki. All animal procedures were performed in accordance with the ARVO Statement for use in ophthalmic and vision research. The study protocol was approved by the Animal Care and Use Committee of the Tongji Hospital, Tongji Medical College, Huazhong University of Science and Technology, China (TJ-IRB20230899). The protocol adhered to the policies and guidelines for the care and use of research animals.

DMEM/F-12 medium was purchased from Gibco (USA). Recombinant human basic fibroblast growth factor (rhFGF-basic) and human leukemia inhibitory factor (hLIF) were obtained from PEPROTECH (USA). Insulin-transferrin-sodium selenite (ITS) media supplement, Collagenase A and Triton X-100 were supplied by Sigma-Aldrich (Germany). 0.25% trypsin containing 1 mM EDTA (T/E) solution and sterile phosphate-buffered saline (PBS) were purchased from Boster Biological Technology Co., Ltd. Dye DiI solution was obtained from Invitrogen (USA). 4% paraformaldehyde fixative was supplied by Sevier Biotechnology Co., Ltd. Normal donkey serum was purchased from Bios Biotechnology Co., Ltd. Mouse monoclonal antibodies against ALDH1A1 and Lumican were obtained from SANTA CRUZ Biotechnology. Mouse monoclonal antibody targeting Laminin was supplied by Boster Biological Technology Co., Ltd. Rabbit polyclonal antibody against Keratocan was purchased from Novus Biologicals. Donkey anti-mouse IgG secondary antibody conjugated with 488 nm green fluorophore, donkey anti-rabbit IgG secondary antibody conjugated with 594 nm red fluorophore, DAPI staining solution and anti-fade mounting medium containing glycerol were all obtained from Bios Biotechnology Co., Ltd. Detailed

information for all primary and secondary antibodies, including manufacturer, catalog number, and working dilution, is provided in Supplementary Table 1.

Single-cell RNA-sequencing

P4 cultured LNC and CSC were used for single-cell RNA seq. Cell suspension was prepared in MESCM following digestion with T/E. Single-cell capture was achieved by BD Rhapsody system and sequenced using Nova seq6000 (Illumina Inc.) on 150 bp paired-end run by Wuhan Ruixing Biotechnology Co., Ltd. Using the Elbow plot method, the principal components were sorted in order of the percentage of variation explained by each. Initial unsupervised clustering using the FindClusters function (resolution = 0.4) identified 10 putative clusters (0-9). Cluster 9 contained fewer than 50 cells with high mitochondrial gene expression (> 20%), indicative of low-quality cells or doublets, and was therefore excluded from downstream analysis. Nine biologically meaningful clusters (0-8) were retained for subsequent annotation and differential expression analysis. UMAP visualization was performed with the same resolution parameter (0.4) on the filtered dataset of 34,959 high-quality cells. The rank-sum test was used to identify differentially expressed genes in various cell types. $Log_2FC > 0.5$ and $P < 0.05$ were considered statistically significant. Passage-4 (P4) cultured LNCs and CSCs were used for scRNA-seq. LNCs were derived from two independent donor corneas (designated LNC_1 and LNC_2, corresponding to donor #1 and donor #2 in **Table 1**), and CSCs were derived from a third donor cornea (donor #3). Of note, LNCs and CSCs were not isolated from matched donor corneas; this design limitation is addressed in the Discussion.

Cell isolation and culturing

Corneas were stored in corneal chamber at 4°C and used within five days. Epithelium, endothelium, and Descemet's membrane were gently scraped off. Rings were sectioned into 12 equal segments and rinsed with PBS. For CSCs: Tissue was incised 1 mm from the limbus on the corneal side, corneal stromal layer was separated. At 37°C under 5% CO_2, the stromal tissue of the transparent cornea was digested using 1 mg/mL Collagenase A for 4-6 hours. Digestion was terminated with serum-containing culture medium. The suspension was centrifuged at 1000 rpm for 5 minutes. The supernatant was discarded, and primary CSCs were harvested. For LNCs: Excess sclera was resected 1 mm from the limbus on the scleral side, limbus tissue was harvested. At 37°C under 5% CO_2, limbal tissue was digested using 1 mg/mL Collagenase A for 8-10 hours, yielding cell clusters. These clusters were further digested with 0.25% trypsin/1 mM EDTA (T/E) for 15 minutes and gently pipetted to achieve complete dissociation into single cells. Digestion was then terminated, and the suspension was centrifuged at 800 rpm for 5 minutes. The supernatant was discarded, and primary LNCs were harvested.

Modified Embryonic Stem Cell Medium (MESCM) was used as the culture medium. Matrigel was diluted with MESCM at a 1:20 ratio to prepare a 5% Matrigel solution. This solution was added to plastic 6-well cell culture plates at 1 mL per well. The plates were incubated undisturbed at 37°C for at least 1 hour. Following incubation, the excess unbound liquid was aspirated, yielding Matrigel-coated plates. MESCM (1 mL) was added to each well of the coated plates. Primary CSCs and primary LNCs were then seeded onto the Matrigel-coated surface at a density of 1×10^4 cells/cm^2. Cell culture was maintained at 37°C under a 5% CO_2 atmosphere. The medium was changed every 2-3 days. When cells reached 80% confluency, they were dissociated using 0.25% trypsin/1 mM EDTA (T/E) and subsequently re-seeded onto freshly coated Matrigel plates for subculturing. Cells from passages 3 to 5 were selected for experiments.

Immunofluorescence

Using a Cytofuge (StatSpin) at 1,000 rpm for 6 min, single cells were produced on slides and were fixed with 4% formaldehyde, permeabilized with 0.02% Triton X-100 and blocked with 2% bovine serum albumin before adding primary antibodies. The secondary antibodies were set up for 45 min, using the necessary isotype-matched nonspecific immunoglobulin G antibodies as controls after the unbound primary antibodies were removed with phosphate-buffered saline. Nuclei were counterstained with DAPI (6-diamidino-2-phenylindole) and images were acquired with a Zeiss LSM 700 microscope. The National Institutes of Health's ImageJ program was used for signal

quantification. Supplementary Table 1 contains a comprehensive list of the primary and secondary antibodies as well as the agents utilized for IF.

Histological staining (Hematoxylin and Eosin, H&E)

Enucleated rabbit eyeballs were fixed in 4% paraformaldehyde for 24-48 h at room temperature. The corneal tissue containing the DiI-labeled injection site was dissected, dehydrated through a graded ethanol series (70%, 80%, 90%, 95%, and 100%), cleared in xylene, and embedded in paraffin. Serial sections of 5 μm thickness were cut using a microtome. For H&E staining, sections were deparaffinized in xylene and rehydrated through descending ethanol concentrations to distilled water. Nuclei were stained with hematoxylin solution for 3-5 min, followed by a rinse in running tap water. Differentiation was performed in 1% hydrochloric acid-alcohol for 2-3 s, after which sections were rinsed in running water and blued in 0.6% ammonia water. After another rinse in running water, sections were immersed in distilled water for 2 min and counterstained with eosin solution for 2-3 min. Sections were then dehydrated in ascending ethanol concentrations, cleared in xylene, and mounted with neutral balsam. Images were acquired using an upright light microscope (Olympus BX53, Japan).

Animals experiments

DiI-stained CSC and LNC suspensions were prepared at a density of 3×10^5 cells/mL. Four healthy adult New Zealand white rabbits (males, 6-8 months old, body weight 2.0-2.4 kg) were purchased from the Experimental Animal Center of Tongji Medical College, Huazhong University of Science and Technology (Wuhan, China; Hubei Zhirat Zhihui Biotechnology Co., Ltd.). Rabbits were housed under standard laboratory conditions (12-h light/dark cycle, 22 ± 2°C, 50-60% humidity) with free access to food and water. The animals were randomly divided into two groups (n = 2 per group): Group 1 was euthanized at 2 weeks post-transplantation, and Group 2 at 4 weeks post-transplantation. Under an operating microscope, a tunnel was created in the corneal stroma using a 30-gauge needle. The right cornea of each rabbit received an intrastromal injection of 100 μL DiI-stained LNC suspension (3×10^5 cells/mL) using a Hamilton microsyringe, while the left cornea received an equal volume of DiI-labeled CSC suspension via the same technique. Immediately after injection, fluorescence images of the surgical eyes were captured using in vivo fluorescence microscopy (Cambridge Research & Instrumentation, Inc., USA), followed by topical application of ofloxacin eye ointment (0.3%; Sinqi Pharmaceutical Co., Ltd., China) to prevent infection. Rabbits in Group 1 were euthanized 2 weeks post-transplantation, and Group 2 rabbits were euthanized at 4 weeks. Enucleated eyes were photographed ex vivo, with areas exhibiting red fluorescence identified and marked for analysis.

For all surgical procedures, rabbits were anesthetized by intramuscular injection of a mixture of ketamine hydrochloride (30 mg/kg body weight; Fujian Gutian Pharmaceutical Co., Ltd., China) and xylazine hydrochloride (5 mg/kg body weight; Shengda Animal Pharmaceutical Co., Ltd., China). Topical proparacaine hydrochloride eye drops (0.5%; Alcon, USA) were applied to the ocular surface for local anesthesia. At the designated endpoints, rabbits were euthanized by intravenous injection of an overdose of pentobarbital sodium (150 mg/kg body weight; Sigma-Aldrich, USA) into the marginal ear vein, followed by confirmation of cardiac arrest and pupillary dilation.

Statistical analysis

All quantitative data are expressed as mean ± standard deviation (mean ± SD). For scRNA-seq data processing, the R statistical environment (v4.2.1) with the Seurat package (v4.3.0) was used. Differentially expressed genes between clusters were identified using the Wilcoxon rank-sum test, with $\log_2$ fold change ($\log_2$FC) > 0.5 and adjusted *P*-value < 0.05 considered statistically significant. For in vitro immunofluorescence quantification, fluorescence intensity was measured using ImageJ software (v1.54f). Comparisons of mean fluorescence intensity between LNC and CSC groups were performed using a two-tailed unpaired Student's t-test in GraphPad Prism (v9.5.0). Significance levels were defined as $*P < 0.05$, $**P < 0.01$, and $***P < 0.001$. Due to the small sample size of the in vivo rabbit experiment (n = 2 per group), no formal inferential statistical testing was applied to cell migration patterns or spatial

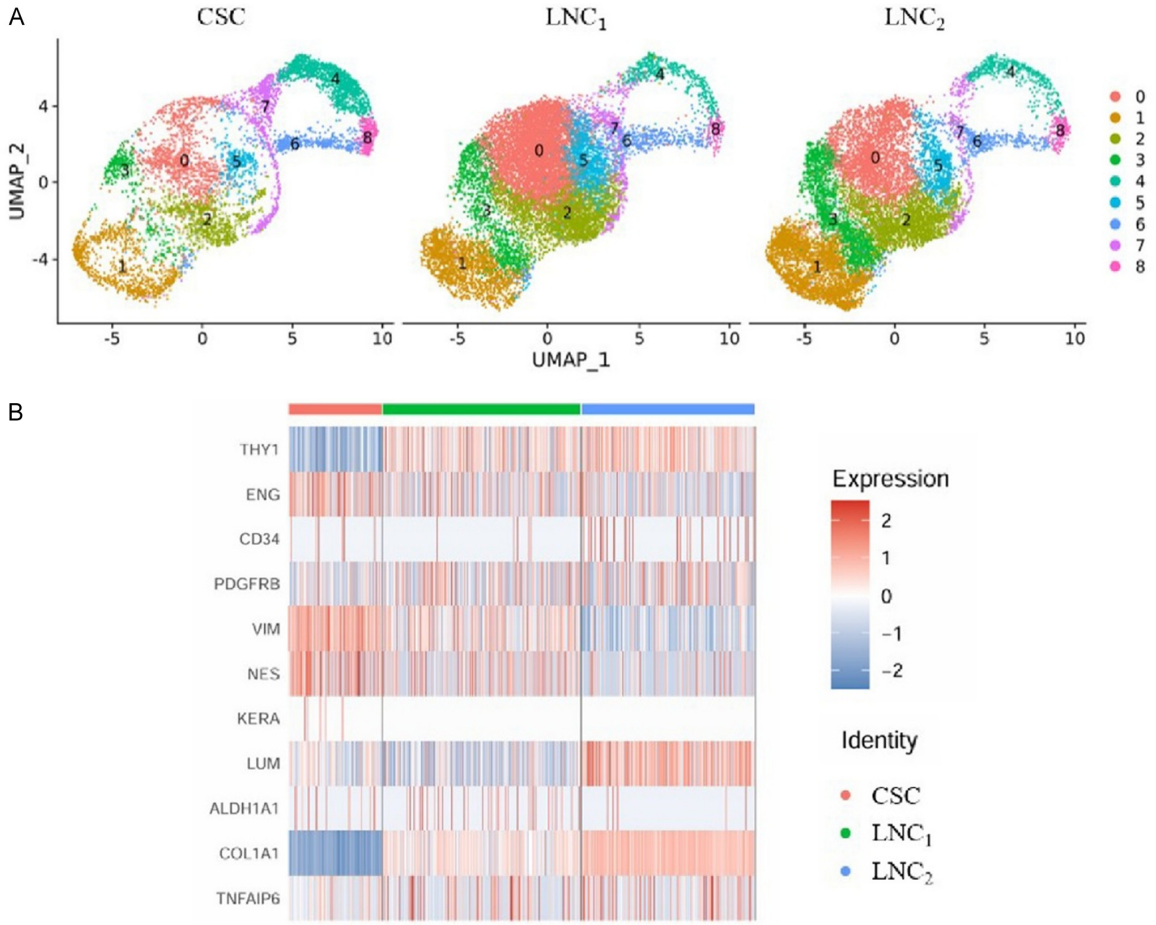


Figure 1. Single-cell transcriptomic profiling of cultured LNCs and CSCs. A. UMAP visualization of 34,959 cells colored by unsupervised clustering (clusters 0-8). LNC_1 and LNC_2 represent scRNA-seq data from two independent LNC donor cultures; CSC represents data from one independent CSC donor culture. Scale: each dot represents one cell. B. Heatmap showing the relative expression levels of selected marker genes across CSC, LNC_1, and LNC_2 samples. Color intensity represents row-scaled normalized expression values (blue, low expression; red, high expression).

distribution data; these results are presented as descriptive qualitative observations.

Result

Single-cell RNA-sequencing

Following scRNA-seq data preprocessing, 34,959 high-quality cell samples were obtained, comprising 27,521 cells from the LNC and 7438 cells from CSC. The Uniform Manifold Approximation and Projection (UMAP) algorithm was used for cornea cell annotation and different cornea markers were shown (**Figure 1A**). The UMAP plots depict the distribution of cell subpopulations in CSC, LNC_1, and LNC_2 samples, where LNC_1 and LNC_2 represent scRNA-seq profiles derived from two independent LNC donor cultures (donor #1 and donor #2 in **Table 1**), respectively. Each color-coded cluster represents a unique cell subpopulation, labeled 0-8. In the CSC sample, cell subpopulations (0-8) formed discrete clusters. Subpopulation 0 exhibited a central distribution, whereas subpopulations 1-8 occupied peripheral regions. For LNC_1 and LNC_2 samples, despite an overall clustering architecture analogous to that of CSC (e.g., subpopulation 0 remained centrally located), notable disparities in subpopulation composition were observed. Specifically, subpopulation 4, relatively abundant in CSC, showed sparser distribution in LNC_1 and LNC_2. Meanwhile, subpopulation 6 displayed altered spatial patterning across the three sample groups. These UMAP results reveal that, while a conserved clustering framework exists among CSC, LNC_1, and LNC_2, dis-

Table 2. Characteristic marker genes distinguishing CSCs and LNCs identified by scRNA-seq differential expression analysis

Grouping	Gene Symbol	Cell Type-Specific Expression Characteristics	Matching Degree of Biological Function with Corneal Tissue
CSC Highly Expressed	VIM	A classic cytoskeletal marker for fibroblast-like corneal stromal cells, highly expressed in activated stromal cells	Stromal cells require high VIM expression to maintain morphology and contractile function, while low expression in LNC is consistent with their relatively quiescent niche cell properties
CSC Highly Expressed	LUM	A specific core marker for corneal stromal cells, involved in the ordered arrangement of collagen fibers in the corneal stroma	LUM is a key protein for maintaining corneal stromal transparency, and low expression in LNC is consistent with its identity as a non-stromal core structural cell
LNC Highly Expressed	THY1 (CD90)	A characteristic surface marker for limbal mesenchymal stem cells/limbal niche cells	Limbal niche cells highly express THY1, which is involved in regulating the stemness maintenance of limbal stem cells and is highly matched with LNC functions

tinct cell subpopulations manifest sample - specific distribution traits.

To characterize the biological identity of each subpopulation, we identified cluster-specific marker genes and performed Gene Ontology (GO) and Kyoto Encyclopedia of Genes and Genomes (KEGG) functional enrichment analyses (Supplementary Table 2). Cluster 0, the most abundant subpopulation across all samples, was enriched for canonical mesenchymal markers including VIM, COL3A1, and DCN, and was associated with extracellular matrix organization and collagen fibril organization, consistent with a stromal fibroblast-like phenotype. Cluster 1 showed high expression of cell-cycle regulators (MKI67, TOP2A, CCNB1) and was enriched for mitotic nuclear division and DNA replication terms, representing a proliferative progenitor subpopulation. Cluster 2 was characterized by elevated expression of stress-response and immediate-early genes (FOS, JUN, ATF3), with functional enrichment in response to oxidative stress and cellular response to stress. Cluster 3 displayed enrichment for immune-modulatory genes (CXCL8, IL6, CCL2) and was associated with cytokine-mediated signaling pathways. Cluster 4, relatively enriched in CSC samples, expressed high levels of mature keratocyte markers including KERA, LUM, and ALDH1A1, with functional annotation in collagen biosynthetic process and corneal transparency maintenance. Cluster 5 showed elevated expression of mesenchymal stem cell markers (THY1, ENG, PDGFRB) and was enriched for mesenchyme development and stem cell population maintenance, likely representing a less-differentiated progenitor state. Cluster 6 was characterized by genes involved in cell migration and motility (MMP2, SERPINE1, PLAU), with enrichment in extracellular matrix disassembly and cell migration terms. Cluster 7 displayed high expression of genes related to protein synthesis and ribosomal biogenesis (RPL genes, RPS genes), suggesting a metabolically active state. Cluster 8 was enriched for angiogenic factors (VEGFA, ANGPT2) and endothelial-associated markers, with functional annotation in blood vessel development and angiogenesis. The full list of cluster-specific marker genes and enrichment results is provided in Supplementary Table 2.

Differential expression analysis revealed distinct transcriptomic profiles between CSC and LNC samples. THY1 (CD90), a canonical mesenchymal stem cell and limbal niche marker, was highly expressed in both LNC_1 and LNC_2 samples but was nearly absent in CSC ($P < 0.001$). In contrast, VIM was strongly expressed in CSC but showed markedly lower expression in LNC samples ($P < 0.001$). LUM, a core corneal stromal proteoglycan, was enriched in CSC relative to LNC ($P < 0.001$). KERA showed low but detectable expression across all samples, with modest enrichment in the CSC-specific cluster 4. ENG and PDGFRB exhibited variable expression across subpopulations, with higher levels in LNC-enriched clusters, consistent with a mesenchymal progenitor phenotype. These differential expression patterns are illustrated in the heatmap (**Figure 1B**).

To identify cell type-specific marker genes distinguishing corneal stromal cells (CSC) from limbal niche cells (LNC), differential gene expression analysis was performed, and the core characteristic genes with consistent biological functions were screened out. As shown in **Table 2**, two genes were specifically highly expressed in CSC, including VIM and LUM. VIM, a classic cytoskeletal marker for fibroblast-like cells, was

highly expressed in activated CSC, which is essential for maintaining the morphological integrity and contractile function of stromal cells - consistent with the functional demand of CSC as the core functional cells in the corneal stroma. In contrast, VIM expression was low in LNC, reflecting the relatively quiescent phenotypic feature of limbal niche cells. Another CSC-specific gene, LUM, serves as a core marker for corneal stromal cells and plays a pivotal role in regulating the ordered arrangement of collagen fibers in the corneal stroma. The high expression of LUM in CSC is closely related to the maintenance of corneal transparency, while its low expression in LNC aligns with LNC's identity as non-stromal structural cells. For LNC, THY1 (CD90) was identified as the key specific marker gene. As a characteristic surface marker for limbal mesenchymal stem cells and niche cells, THY1 is highly expressed in LNC and participates in the regulation of stemness maintenance of limbal stem cells, which is consistent with the core functional role of LNC in constructing the limbal stem cell niche. Collectively, VIM and LUM can be used as specific marker genes for CSC, while THY1 is a reliable marker for LNC, providing valuable molecular targets for the identification and functional research of these two cell populations in corneal tissue engineering and regenerative medicine.

Morphological comparison between LNCs and CSCs

Both LNCs and CSCs can adhere to the culture substrate within 24 hours. Under high-power microscopy, there are both similarities and differences in the adhesion morphology of the two types of cells. It can be seen that LNCs are in the shape of slender spindles or fusiforms, while the cells in the proliferative state are shorter and smaller with higher brightness under the microscope. On the 3rd day of culture, some of the adherent CSCs are spindle-shaped, showing the morphology of fibroblasts, which is similar to that of LNCs, and some are dendritic, which is their typical morphology in vivo. With cell proliferation and passage, the CSCs cultured until the 6th day gradually lose their original dendritic morphology and all present slender spindle or fusiform shapes similar to those of LNCs (**Figure 2A**).

Immunofluorescence

Cytospin immunofluorescence staining demonstrated that both LNCs and CSCs expressed all four markers. Among them, Lumican, ALDH1A1, and Keratocan were expressed in the cytoplasm, while Laminin was expressed in both the cytoplasm and nucleus. The fluorescence intensity of Lumican and ALDH1A1 in LNCs was weak, whereas CSCs showed strong positive expression of these two markers. There was no significant difference in the expression intensity of Keratocan and Laminin between the two types of cells (**Figure 2B**).

The average fluorescence intensity per cell of the two cell types was measured using ImageJ software. Quantitative analysis using ImageJ demonstrated that the mean fluorescence intensity of Lumican was significantly lower in LNCs than in CSCs ($P < 0.001$, two-tailed unpaired t-test). ALDH1A1 intensity was also significantly reduced in LNCs compared with CSCs. No significant differences were observed for Keratocan ($P = 0.582$) or Laminin ($P = 0.634$) between the two cell types (**Figure 2C**).

In vivo survival and distribution of transplanted cells in rabbit corneas

LNCs and CSCs were labeled with DiI dye and injected into the stromal layer of the right and left eyes of two groups of rabbits, respectively. In vivo fluorescence microscopy was used for imaging. The rabbits were further raised for 2 and 4 weeks, then sacrificed, and their eyeballs were harvested for observation of red fluorescent signals under in vivo fluorescence microscopy. In the right eyes of both groups of rabbits injected with LNCs, the fluorescent signals appeared as punctate red fluorescence. No significant changes in fluorescence intensity or distribution pattern were observed after 2 and 4 weeks of culture (**Figure 3Aa**, **3Ab**, **3Ae**, **3Af**).

The CSCs injected into the left eyes showed strong fluorescent signals. In the left eye of the first group of rabbits, the red fluorescence matched the shape of the needle puncture tract, and there was no significant change in the cell distribution pattern after 2 weeks of culture compared with that at the time of injection (**Figure 3Ac**, **3Ad**). In the left eye of the second group of rabbits, the red fluorescence

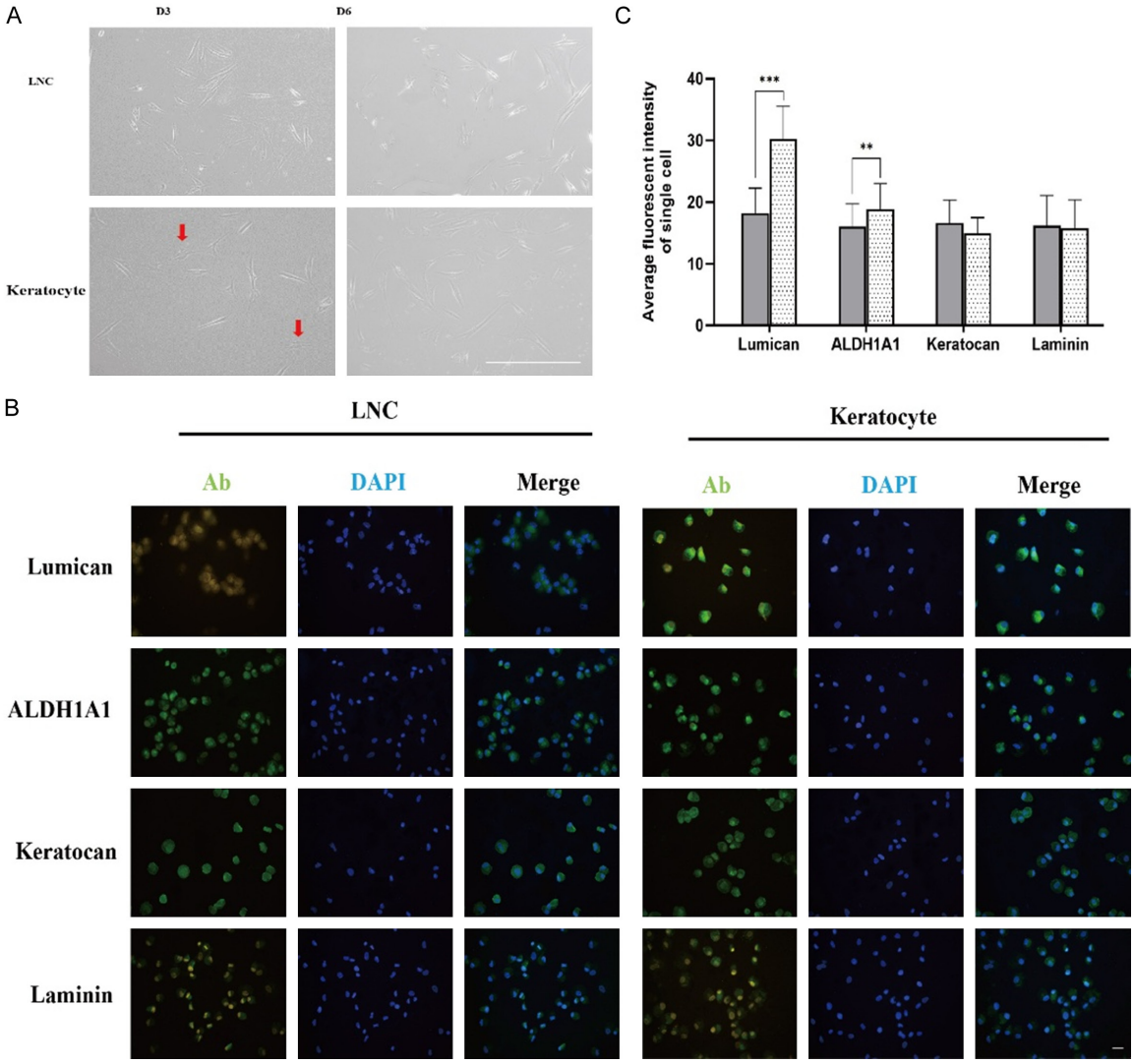


Figure 2. Morphological and immunophenotypic comparison of LNCs and CSCs in vitro. A. Phase-contrast microscopy showing morphological changes of LNCs and CSCs at days 3 and 6 of culture. Original magnification: ×100; scale bar = 100 μm. B. Immunofluorescence staining of Lumican, ALDH1A1, Keratocan, and Laminin in LNCs and CSCs. Green fluorescence indicates antibody staining; blue fluorescence (DAPI) indicates cell nuclei. Original magnification: ×400; scale bar = 20 μm. C. Quantitative analysis of mean fluorescence intensity per cell for Lumican, ALDH1A1, Keratocan, and Laminin. Data are presented as mean ± SD from three independent experiments; **P < 0.01, ***P < 0.001 (two-tailed unpaired Student's t-test).

of CSCs was in the form of clumps, and after 4 weeks of culture, the fluorescent signal showed a tendency to spread outward compared with that at the time of injection (**Figure 3Ag**, **3Ah**). These descriptive observations suggest that both LNCs and CSCs can survive for at least 4 weeks in the rabbit corneal stroma after intrastromal injection, and that CSCs may exhibit a greater tendency for stromal migration compared with LNCs. Two groups of rabbits that underwent cell transplantation were sacrificed at 2 weeks and 4 weeks respectively, and their eyeballs were harvested. The eyeballs were fixed in 4% paraformaldehyde, embedded in paraffin, and sectioned at the DiI-labeled sites. HE staining was performed on the sections. The corneas in HE-stained sections from both groups of rabbits injected with LNC cell suspension and corneal stromal cell suspension showed good integrity, with no obvious stromal scarring observed by naked eye (**Figure 3B**).

Rabbits from the two cell transplantation groups were sacrificed at 2 and 4 weeks, respectively. At 4 weeks post-transplantation,

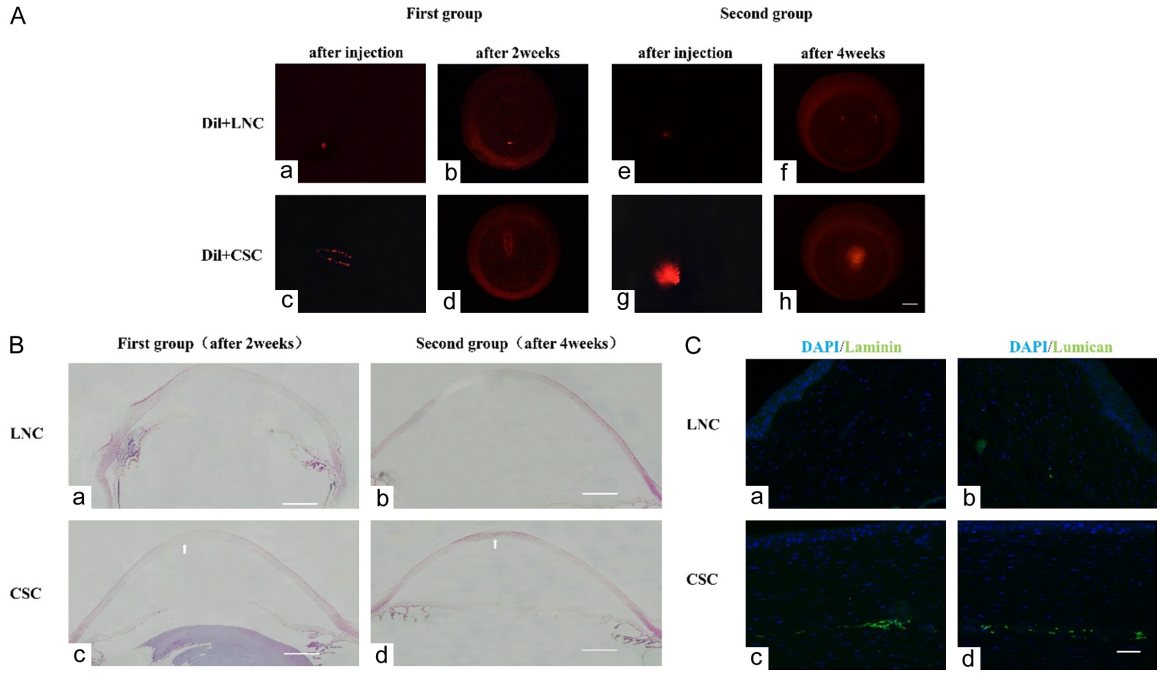


Figure 3. In vivo survival and distribution of transplanted LNCs and CSCs in rabbit corneas. A. In vivo fluorescence tracking of DiI-labeled LNCs (right eye) and CSCs (left eye) at 2 weeks (Group 1) and 4 weeks (Group 2) post-transplantation. Red fluorescence indicates DiI-labeled cells. Original magnification: ×12.5; scale bar = 2 mm. B. H&E staining of corneal sections at 2 and 4 weeks after LNC or CSC transplantation, showing stromal architecture and absence of scarring. Original magnification: ×40; scale bar = 500 μm. C. Immunofluorescence staining of Lumican in corneal sections at 4 weeks post-transplantation. Green fluorescence indicates Lumican expression; blue fluorescence (DAPI) indicates cell nuclei. Original magnification: ×400; scale bar = 20 μm.

eyeballs sections were subjected to Lumican immunofluorescent staining, and DiI-positive regions were imaged using fluorescence microscopy. In the right eye sections, scattered Lumican fluorescent signals with relatively strong intensity were observed, indicating that a small number of LNCs survived in the rabbit corneal stroma and were capable of expressing Lumican. In the left eye sections, strongly positive Lumican fluorescence signals were distributed in a layered arrangement, demonstrating that more CSCs survived in the rabbit corneal stroma and expressed Lumican (**Figure 3C**). Combined with the results of DiI staining fluorescence in rabbit eyes, CSCs appeared to arrange in layers within the stroma, with a potential tendency for parallel migration but no migration toward the epithelium or anterior chamber.

Discussion

This study provides a comprehensive analysis of LNCs and CSCs through integrated transcriptomic, morphological, and in vivo assessments, revealing their shared characteristics and key differences that inform potential lineage conversion strategies.

Transcriptomic Insights and lineage relationships

Our in vivo data demonstrating long-term cell viability without inflammatory reaction or stromal scarring support the safety of LNC transplantation in the corneal stroma. When evaluating LNCs as a seed cell source for corneal stromal regeneration, it is instructive to compare their unique advantages against alternative cell types that have been investigated for this purpose. Our scRNA-seq analysis identified distinct clustering patterns between LNCs and CSCs, with subpopulation-specific enrichment reflecting their functional specialization. Prior research has explored multiple cells sources for transdifferentiation into corneal stromal cell, including bone marrow mesenchymal stem cells (BMMSCs), adipose-derived mesenchymal stem cells, corneal stromal stem cells, and limbal epithelial progenitors [14-16]. Numer-

ous studies have verified that BMMSCs possess the capacity to differentiate into corneal stromal cells, whereas uninduced BMMSCs show remarkable disparities with native CSCs in marker expression, barely expressing core matrix proteins such as Lumican and Keratocan required for corneal transparency. In vivo transplantation experiments confirmed that the corneal stromal microenvironment could induce BMMSCs to upregulate Keratocan and Lumican, endowing them with CSC-like phenotypes to repair stromal defects; three-dimensional in vitro induction systems further validated that directional culture significantly elevated the expression of CSC-specific factors including ALDH1A1 and Lumican in BMMSCs, realizing the conversion toward keratocyte lineage [17, 18]. In these transdifferentiation systems, researchers defined classic CSC signature antigens as Lumican, Keratocan, ALDH1A1, Vimentin, while surface markers like PDGFRβ were also widely used to identify mature stromal keratocytes [14, 17, 19-21].

LNCs offer several unique advantages over these alternative seed cell sources. First, LNCs share anatomical and developmental homology with the corneal stroma: both LNCs and CSCs are derived from the neural crest and reside within the corneal/limbal stromal compartment, potentially requiring less extensive epigenetic reprogramming to achieve a CSC phenotype compared with non-ocular MSCs. Second, LNCs can be isolated from limbal tissue obtained during routine corneal transplantation procedures, avoiding the need for invasive extra-ocular tissue harvesting. Third, our scRNA-seq data demonstrate that LNCs constitutively express a subset of corneal stromal markers (Keratocan, Laminin) at baseline, indicating a pre-existing transcriptional proximity to CSCs that is not observed in BMMSCs or ADSCs. Fourth, LNCs retain robust expression of mesenchymal progenitor markers (CD73, CD90/THY1, CD105) and neural crest markers, conferring high differentiation plasticity. Finally, the in vivo safety profile observed in our rabbit model - with no evidence of inflammation, rejection, or scarring at 4 weeks - supports the feasibility of LNC-based stromal cell therapy.

Morphological plasticity and functional implications

The spindle-shaped morphology adopted by both cell types following prolonged culture suggests inherent plasticity that may be exploited for therapeutic purposes. This phenotypic convergence, potentially mediated by Matrigel-induced niche mimicry, mirrors observations that CSCs modulate their shape to regulate matrix synthesis [22]. Notably, the dendritic-to-spindle transition observed in CSCs correlates with enhanced migratory capacity, supported by PDGFRβ expression - a marker linked to directed stromal cell migration in wound healing [23].

The conserved expression of Keratocan and Laminin across both cell types indicates shared roles in maintaining corneal structural integrity, while their differential spatial distribution in vivo underscores functional specialization. This aligns with proteomic studies identifying core ECM networks that preserve corneal transparency.

Therapeutic potential and clinical relevance

Our in vivo data demonstrating long-term viability without scarring builds upon previous reports of cell-based therapies for corneal disorders. Compared to adipose-derived stem cells currently used in keratoconus treatment, LNCs offer advantages due to their corneal specificity and inherent capacity for stromal integration [24]. The punctate distribution of LNCs versus layered migration of CSCs suggests that successful conversion would require inducing migratory capabilities through targeted regulation of pathways such as PDGF-BB signaling, which promotes non-fibrotic stromal repair.

The retained expression of mesenchymal markers in transplanted LNCs supports their potential to acquire CSC-like functions in vivo, particularly in the context of ECM remodeling. This has significant implications for treating conditions like keratoconus, where stromal thinning and irregularity result from impaired matrix homeostasis.

This study's limitations include the small sample size of donor tissues and short-term follow-up in animal models. Future investigations should: explore mechanosensitive pathways (YAP1/TEAD1) and growth factor signaling (TGF-β, PDGF) identified in proteomic studies to drive LNC differentiation; Utilize 3D culture systems that mimic the limbal niche, which

have been shown to maintain LNC stemness and enhance differentiation potential; Validate findings in keratoconus models to assess functional restoration of stromal biomechanics [25]; Investigate epigenetic regulators of lineage-specific gene expression, particularly those governing ECM organization.

Limitations and future directions

Several limitations of this study should be acknowledged. First, the scRNA-seq analysis was performed on LNCs and CSCs derived from different donor corneas (two donors for LNC and one donor for CSC), rather than from matched donor pairs. Inter-individual genetic and environmental variation may therefore contribute to some of the observed transcriptomic differences between the two cell types. Future studies using LNCs and CSCs isolated from the same matched donor corneas will be necessary to confirm cell-type-specific expression signatures independent of donor variability. Second, the in vivo rabbit transplantation experiment included a small sample size (n = 2 rabbits per time point, total N = 4), which precluded formal statistical testing of cell migration patterns and spatial distribution differences. The in vivo results should therefore be interpreted as preliminary qualitative observations, and larger animal cohorts with quantitative image analysis are warranted for robust validation. Third, the follow-up period was limited to 4 weeks; long-term studies assessing cell survival, integration, and corneal transparency maintenance over several months are needed.

Future investigations should: (i) explore mechanosensitive pathways (YAP1/TEAD1) and growth factor signaling (TGF-β, PDGF-BB) to drive efficient LNC-to-CSC differentiation; (ii) utilize 3D culture systems that mimic the limbal niche microenvironment to maintain LNC stemness and enhance differentiation potential; (iii) validate functional restoration of stromal biomechanics in keratoconus models; and (iv) investigate epigenetic regulators governing lineage-specific gene expression, particularly those controlling ECM organization and collagen fibrillogenesis.

Conclusion

Our multi-dimensional analysis establishes LNCs as a viable precursor for CSC regeneration, with implications for developing cell-based therapies for corneal stromal disorders. By bridging transcriptomic profiles with functional assays, this work provides a framework for future studies aimed at harnessing LNC plasticity to restore corneal transparency in conditions characterized by stromal dysfunction.

Acknowledgements

The authors thank the Red Cross Eye Bank at Tongji Hospital for providing human corneal tissues. We also thank the staff of the Hubei Key Laboratory of Otorhinolaryngologic and Ophthalmic Diseases for technical support. This study was supported by grants from the National Natural Science Foundation of China (82471050, 82070936), the Ministry of Science and Technology of China (S20240235), and the Science and Technology Talent Service Enterprise Project of Department of Science and Technology of Hubei Province (2024DJC066).

Disclosure of conflict of interest

None.

Address correspondence to: Drs. Guigang Li and Lingjuan Xu, Department of Ophthalmology, Tongji Hospital, Tongji Medical College, Huazhong University of Science and Technology, 1095 Jiefang Road, Qiaokou District, Wuhan 430030, Hubei, China. E-mail: guigangli@hust.edu.cn (GGL); xlj_doc@163.com (LJX)

References

[1] Pellegrini G, Golisano O, Paterna P, Lambiase A, Bonini S, Rama P and De Luca M. Location and clonal analysis of stem cells and their differentiated progeny in the human ocular surface. J Cell Biol 1999; 145: 769-82.

[2] Thoft RA and Friend J. The X, Y, Z hypothesis of corneal epithelial maintenance. Invest Ophthalmol Vis Sci 1983; 24: 1442-3.

[3] Bibak-Bejandi Z, Arabpour Z, Razavi A, Moghtader A, Shahjahan S, Alzein A, Kwon JE, Bibak-Bejandi R, Aly N and Djalilian A. Limbal stem cell deficiency approaches and limbal niche restoration. Indian J Ophthalmol 2025; 73: 468-482.

[4] Bonnet C, Gonzalez S and Deng SX. Limbal stem cell therapy. Curr Opin Ophthalmol 2024; 35: 309-314.

[5] Bonnet C, González S, Roberts JS, Robertson SYT, Ruiz M, Zheng J and Deng SX. Human limbal epithelial stem cell regulation, bioengineering and function. Prog Retin Eye Res 2021; 85: 100956.
[6] Moreno IY, Parsaie A, Gesteira TF and Coulson-Thomas VJ. Characterization of the limbal epithelial stem cell niche. Invest Ophthalmol Vis Sci 2023; 64: 48.
[7] Robertson SYT, Roberts JS and Deng SX. Regulation of limbal epithelial stem cells: importance of the niche. Int J Mol Sci 2021; 22: 11975.
[8] Matthyssen S, Van den Bogerd B, Dhubhghaill SN, Koppen C and Zakaria N. Corneal regeneration: a review of stromal replacements. Acta Biomater 2018; 69: 31-41.
[9] Hay ED. Development of the vertebrate cornea. Int Rev Cytol 1980; 63: 263-322.
[10] Lynch AP, O'Sullivan F and Ahearne M. The effect of growth factor supplementation on corneal stromal cell phenotype in vitro using a serum-free media. Exp Eye Res 2016; 151: 26-37.
[11] Lakshman N and Petroll WM. Growth factor regulation of corneal keratocyte mechanical phenotypes in 3-D collagen matrices. Invest Ophthalmol Vis Sci 2012; 53: 1077-86.
[12] Kim A, Lakshman N, Karamichos D and Petroll WM. Growth factor regulation of corneal keratocyte differentiation and migration in compressed collagen matrices. Invest Ophthalmol Vis Sci 2010; 51: 864-75.
[13] Singh V, Barbosa FL, Torricelli AA, Santhiago MR and Wilson SE. Transforming growth factor β and platelet-derived growth factor modulation of myofibroblast development from corneal fibroblasts in vitro. Exp Eye Res 2014; 120: 152-60.
[14] Dos Santos A, Balayan A, Funderburgh ML, Ngo J, Funderburgh JL and Deng SX. Differentiation capacity of human mesenchymal stem cells into keratocyte lineage. Invest Ophthalmol Vis Sci 2019; 60: 3013-3023.
[15] Basu S, Hertsenberg AJ, Funderburgh ML, Burrow MK, Mann MM, Du Y, Lathrop KL, Syed-Picard FN, Adams SM, Birk DE and Funderburgh JL. Human limbal biopsy-derived stromal stem cells prevent corneal scarring. Sci Transl Med 2014; 6: 266ra172.
[16] Yan Y, Cao Y, Cheng R, Shen Z, Zhao Y, Zhang Y, Zhou G and Sang S. Preparation and in vitro characterization of gelatin methacrylate for corneal tissue engineering. Tissue Eng Regen Med 2022; 19: 59-72.
[17] Liu H, Zhang J, Liu CY, Hayashi Y and Kao WW. Bone marrow mesenchymal stem cells can differentiate and assume corneal keratocyte phenotype. J Cell Mol Med 2012; 16: 1114-24.
[18] Taoum A, Friede R, Thaden O, Rachynskyi O, Frank A, Wang M, Dehli F, Fuest M and Duarte Campos D. 3D differentiation of bone-marrow derived mesenchymal stromal cells into the keratocyte lineage for corneal bioprinting. Adv Healthc Mater 2025; 14: e2405073.
[19] Alió Del Barrio JL and Alió JL. Cellular therapy of the corneal stroma: a new type of corneal surgery for keratoconus and corneal dystrophies. Eye Vis (Lond) 2018; 5: 28.
[20] Karamichos D, Funderburgh ML, Hutcheon AE, Zieske JD, Du Y, Wu J and Funderburgh JL. A role for topographic cues in the organization of collagenous matrix by corneal fibroblasts and stem cells. PLoS One 2014; 9: e86260.
[21] Branch MJ, Hashmani K, Dhillon P, Jones DR, Dua HS and Hopkinson A. Mesenchymal stem cells in the human corneal limbal stroma. Invest Ophthalmol Vis Sci 2012; 53: 5109-16.
[22] Menasche M, Savoldelli M and Pouliquen Y. The keratocyte or fibroblast of the cornea: morphological and biochemical characteristics in normal stroma and a few cases of corneal dystrophies. Pathol Biol (Paris) 1992; 40: 871-8.
[23] Gallego-Muñoz P, Ibares-Frías L, Garrote JA, Valsero-Blanco MC, Cantalapiedra-Rodríguez R, Merayo-Lloves J and Carmen Martínez-García M. Human corneal fibroblast migration and extracellular matrix synthesis during stromal repair: role played by platelet-derived growth factor-BB, basic fibroblast growth factor, and transforming growth factor-β1. J Tissue Eng Regen Med 2018; 12: e737-e746.
[24] Kureshi AK, Dziasko M, Funderburgh JL and Daniels JT. Human corneal stromal stem cells support limbal epithelial cells cultured on RAFT tissue equivalents. Sci Rep 2015; 5: 16186.
[25] Dou S, Wang Q, Zhang B, Wei C, Wang H, Liu T, Duan H, Jiang H, Liu M, Qi X, Zhou Q, Xie L, Shi W and Gao H. Single-cell atlas of keratoconus corneas revealed aberrant transcriptional signatures and implicated mechanical stretch as a trigger for keratoconus pathogenesis. Cell Discov 2022; 8: 66.

Supplementary Table 1. Antibodies and reagents used in this study

Antibody/Reagent	Target/Specificity	Manufacturer	Catalog No.	Working dilution/concentration
Anti-ALDH1A1 (mouse mAb)	ALDH1A1	Santa Cruz Biotechnology	sc-374149	1:200
Anti-Lumican (mouse mAb)	Lumican	Santa Cruz Biotechnology	sc-166862	1:100
Anti-Laminin (mouse mAb)	Laminin	Boster Biological Technology	BM0085	1:100
Anti-Keratocan (rabbit pAb)	Keratocan	Novus Biologicals	NBP1-88804	1:100
Donkey anti-mouse IgG (H+L), Alexa Fluor 488	Mouse IgG	Bios Biotechnology Co., Ltd.	BF06001	1:500
Donkey anti-rabbit IgG (H+L), Alexa Fluor 594	Rabbit IgG	Bios Biotechnology Co., Ltd.	BF07002	1:500
DAPI staining solution	DNA/nuclei	Bios Biotechnology Co., Ltd.	AR1176	1:1000
DiI (CellTracker CM-DiI)	Cell membrane	Invitrogen/Thermo Fisher	C7000	2 μM
Collagenase A	Collagen digestion	Sigma-Aldrich	10103586001	1 mg/mL
DMEM/F-12 medium	Cell culture	Gibco/Thermo Fisher	11320033	Undiluted (working medium)
rhFGF-basic	bFGF	PeproTech	100-18B	10 ng/mL
hLIF	LIF	PeproTech	300-05	10 ng/mL
ITS supplement	Insulin-Transferrin-Selenium	Sigma-Aldrich	I3146	1:100 (1X)

Supplementary Table 2. Cluster-specific marker genes and functional enrichment analysis for clusters 0-8

Cluster	Top Marker Genes	GO Biological Process Enrichment	Putative Cell Identity
0	VIM, COL3A1, DCN, COL1A1	Extracellular matrix organization; collagen fibril organization	Mature stromal fibroblast-like
1	MKI67, TOP2A, CCNB1, PCNA	Mitotic nuclear division; DNA replication; cell cycle	Proliferative progenitor
2	FOS, JUN, ATF3, HSPA1A	Response to oxidative stress; cellular response to stress	Stress-response subpopulation
3	CXCL8, IL6, CCL2, NFKBIA	Cytokine-mediated signaling; inflammatory response	Immune-modulatory
4	KERA, LUM, ALDH1A1, COL5A1	Collagen biosynthetic process; corneal transparency maintenance	Mature keratocyte (CSC-enriched)
5	THY1, ENG, PDGFRB, NT5E	Mesenchyme development; stem cell population maintenance	Mesenchymal progenitor (LNC-enriched)
6	MMP2, SERPINE1, PLAU, TIMP1	Extracellular matrix disassembly; cell migration	Migratory/remodeling
7	RPL10, RPS24, RPL13, EEF1A1	Ribosome biogenesis; translation; protein folding	Metabolically active
8	VEGFA, ANGPT2, KDR, PECAM1	Blood vessel development; angiogenesis	Angiogenic/endothelial-like